Hindawi
Science and Technology of Nuclear Installations
Volume 2018, Article ID 2631084, 9 pages
https://doi.org/10.1155/2018/2631084

Research Article

Temperature Profile Measurement in Simulated Fuel Assembly Structure with Wire-Mesh Technology

Hiroki Takiguchi, Masahiro Furuya, and Takahiro Arai

Central Research Institute of Electric Power Industry, 240-0196, Japan

Correspondence should be addressed to Hiroki Takiguchi; t-hiro@criepi.denken.or.jp

Received 22 April 2018; Revised 25 July 2018; Accepted 1 November 2018; Published 13 November 2018

Academic Editor: Michel Giot

When light water reactor (LWR) is subject to a cold shutdown, it needs to be cooled with pure water or seawater to prevent the core melting. To precisely evaluate the cooling characteristics in the fuel assembly, a measurement method capable of installing to the fuel assembly structure and determining the temperature distribution with high temporal resolution, high spatial resolution, and in multidimension is required. Furthermore, it is more practical if applicable to a pressure range up to the rated pressure 16 MPa of a pressurized water reactor (PWR). In this study, we applied the principle of the wire-mesh sensor technology used in the void fraction measurement to the temperature measurement and developed a simulated fuel assembly (bundle) test loop with installing the temperature profile sensors. To investigate the measurement performance in the bundle test section, it was confirmed that a predetermined temperature calibration line with respect to time-average impedance was calculated and became a function of temperature. To evaluate the followability of measurement in a transient temperature change process, we fabricated a 16 × 16 wire-mesh sensor device and measured the hot-water jet-mixing process into the cold-water pool in real time and calculated the temperature profile from the temperature calibration line obtained in advance from each measurement point. In addition, the sensors applied to three-dimensional temperature distribution measurement of a complex flow field in the bundle structure. The axial and cross-sectional profiles of temperature were quantified in the forced flow field with nonboiling when the 5×5 bundle was heated by energization.

1. Introduction

To quantify the thermoreactive flow field for some industrial applications such as column, chemical, and nuclear reactors, high tempospatial measurements for temperature, pressure, phasic velocity, and void fraction are required. In the case of void-fraction measurement, F. Wang et al. measured the volumetric void fraction of a gas-liquid vertical flow with dynamic differential pressure and quantitatively estimated the determination error [1]. F. Chen et al. applied an optical fiber probe to detect the averaged cross-sectional void fraction of a vertically rising two-phase flow in oil pipes [2] and M. E. Shawkat also selected the same optical fiber technique to compare with a hot-film anemometry [3]. H. M. Prasser et al. compared the void-fraction measurement in a vertical pipe between an ultra-fast X-ray CT and a wire-mesh sensor [4], while S. Hosokawa et al. selected laser Doppler velocimetry (LDV) to evaluate bubble-induced pseudo turbulence in a two-phase laminar flow in a vertical pipe [5]. Some ready-made and conventional methods have both merits and demerits. For example, although the differential pressure technique can measure with high-speed performance, the detected information is limited to only spatial averaged value. Conversely, the optical probe apparatus can access inner volumetric areas with high void fractions in which a high-speed camera would be unable to visualize, but the technique is limited to a point measurement. It is crucial to develop measurement techniques which retain compatibility between multidimensionality and real-time performance and with that, in mind, the wire-mesh technology has these characteristics. H. M. Prasser et al. [6] provided an innovative technique measuring multidimensional void fraction and gas-phase velocity at high time resolution, so-called "wire-mesh sensor" (WMS). WMS can demarcate gas and liquid-phases

based on the difference in terms of gap impedance between two wires. By adopting the WMS principle, the authors' group previously developed a subchannel void sensor (SCVS) [7], a liquid film sensor [8], and a predictive technique of 3D velocity vector [9]. J. Kickhofel et al. [10] applied the sensor to temperature profile measurement for T-junction cross-flow mixing with thermally driven density stratification. As a result, it was clarified that the temperature distribution behavior which is mixed at a temperature difference of 232 K under high pressure of 7 MPa can be quantified when coolant supplied from each pipe. When quantifying the thermoreactive field, the fluid temperature in particular has a dominant effect on how the heat transfer and chemical reaction occur. In a steady-state temperature field, an optical or electric probe can be inserted and moved into the test fluid to measure the temperature profile. However, where significant time variation is involved, it is important to obtain its thermal change instantly without disturbing the thermal field. Although laser-induced fluorescence (LIF), which measures temperature with fluorescence intensity from the target fluid, is well known as a high time-resolution method of temperature distribution [11], the optical observation with a laser sheet is difficult because nuclear and chemical reactors are almost always operated under high pressure. A method of measuring temperature profile capable of withstanding high pressure is required, and the WMS technology is suitable from the previous knowledge [10]. Here, this paper focuses on the application of WMS technology for measurement of temperature in a complex reactor core structure of LWR. When the LWR is subject to an emergency cold shutdown, pure water or seawater is injected to cool the reactor core. In evaluating the cooling safety performance of the coolant, there is a need to determine the three-dimensional thermal diffusion behavior in the fuel assembly and a sensor capable of measuring the three-dimensional temperature distribution in the fuel assembly in real time is required, although no measurement examples have been found to date. This paper applies WMS technology as a means of measuring the temperature and developed a bundle test loop with installing the temperature profile sensors. In addition, an applicability test to three-dimensional temperature distribution (cross-sectional direction and vertical direction) for the complex flow path in the bundle structure and a followability test of measurement in a transient thermal change process less than 100°C were demonstrated.

2. Purpose of Sensor Development

The practical purpose of sensor development is to reproduce the scenario of decreasing water level of coolant which may cause core melting in our bundle test facility and to measure accurately the three-dimensional temperature profile of the coolant using pressure and temperature as parameter. As an extension of this tool development, the purpose of this study is to structure a thermal hydraulic database that contributes to core safety design to prevent core melting. In that respect, as mentioned above, J. Kickhofel et al. [10] showed that temperature measurement by WMS technology can be applied under high pressure. On the other hand, the position of this study is to quantify the temperature distribution behavior of coolant in the fuel assembly (core) and to clarify the applicability of WMS technology. In order to realize this object, the following problems need to be solved:

(1) As a novelty from the previous research, it is required to construct a WMS for temperature measurement in combination with the bundle test section and realize fluid temperature measurement within a distance of only 3 mm between simulated rods.

(2) It is required for safety assessment to grasp the heat transfer variation during core cooling at high time resolution on the order of milliseconds and it is necessary to evaluate the applicability of the WMS.

(3) Furthermore, in order to grasp this cooling performance throughout the effective heating area in reactor core of LWR, it is required to be able to measure the temperature distribution of the coolant for the bundle in the cross-sectional direction and in the height direction on a meter scale.

In this experiment, we will prepare a test facility for confirming the above contents and introduce the sensor and clarify the applicability of the temperature distribution in the bundle to the measurement in the cross section and the axial direction and the applicability of the time resolution. The experimental pressure is the atmospheric pressure. It is desirable to evaluate in the atmospheric pressure region [10] where the relationship between the conductivity and the sensor signal becomes linear when evaluating the sensor in bundle.

3. Principles and Apparatus

The third chapter indicates the principle of the temperature measurement technique using WMS technology and two types of our experimental apparatus. To confirm the verification of the principle in a bundle test section and the performance of time resolution in a transient thermal change process, a 5×5 bundle geometry (flow setting) which sets 6×6 wire-mesh structure and a 16×16 wire-mesh sensor (nonflow/pool setting) were respectively prepared. Here, the bundle means a dummy fuel assembly, with twenty five dummy fuel rods set into the test section. Additionally, the nonflow setting means a closed structure to store water, while conversely the former apparatus includes flowing water and temperature regulation functions using a pump, preheater, and condenser.

3.1. Temperature Measuring Method. The measurement principle employs that of the WMS [6, 10]. To design wire electrodes comprising a squared-grid structure at the thermal field, a transmitter wire is orthogonally crossed to another receiver wire while retaining a certain distance in the order of sub-millimeters from each other. Figure 1 shows a schematic image of the temperature measurement principle. The transmitter wire electrodes, which are placed parallel to each other in a north-south direction, have bipolar pulsed inputs applied through some switches (S1, S2, ...in Figure 1) with a voltage

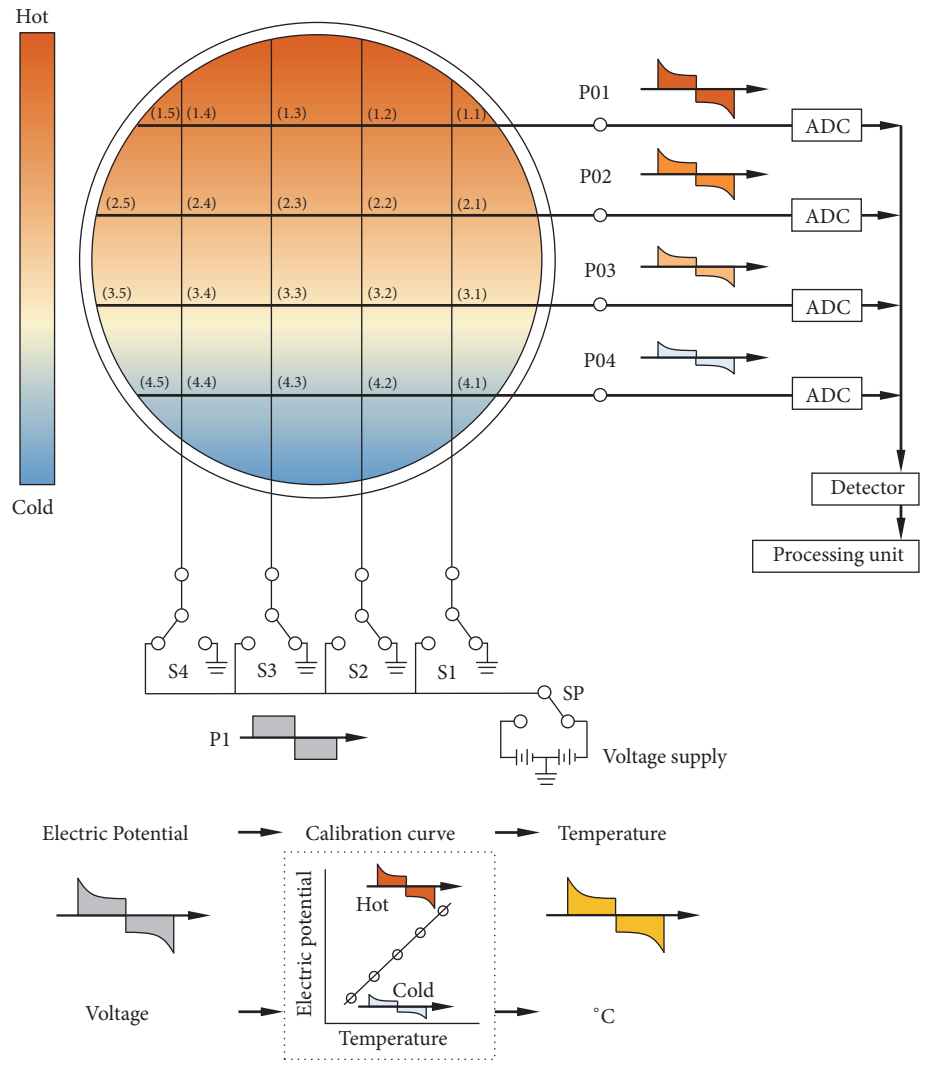

Figure 1: Principle of the temperature profile sensor and its signal processing method.

supply. The volume-averaged electrical impedance of the spatial area sandwiched between the transmitter and receiver wires correlates with the electrical conductivity of this test area. The detected signals (PO1, PO2, ... in Figure 1) from the receiver wires, which are placed parallel to each other in an east-west direction, are delivered to the signal detector and have information reflecting the effect of the electrical impedance of the test area in the test area between the two wires. The WMS principle means that the temperature profile in water can be measured by calculating with the detected signals using a processing unit. In this technique, for which wire-mesh technology is applied, multidimensional and high-speed measurement of the temperature profile is possible in the order of milliseconds by switching them as rapidly as possible. In this experiment, pure water was employed because it is aimed at evaluation of temperature behavior of coolant in the bundle, and however the test fluid is not limited to water.

With the measurement control system illustrated in Figure 1, a calibration line or curve, which is predetermined from the relationship between electrical impedance, namely, the detected sensor signal with the temperature of the test sample and the proofreading of the fluid temperature, was employed with a thermocouple. Accordingly, the determination error of the thermometer is accurate to within ±0.1°C. The calibration trend in this experiment refers to the next chapter. To prevent overlapping of multimeasuring parameters with mutually equivalent sensitivities in terms of temperature measurement, there is a need to keep measuring parameters other than temperature constant, because the electrical impedance of water depends on the distance between transmitter and receiver wires, pH and dissolved oxygen (DO) etc. In the case of a thermal field with a temperature gradient in the north-south direction, as shown in Figure 1, the electrical impedance of water positively correlates with the temperature dependence on electrical conductivity of the same.

The advantage of this measurement method is that it is the maximum merit that it can be applied under high pressure [10] unlike the visualization and laser method, but on the other hand, the spatial resolution is considered to be constrained by the distance between wires. It is possible

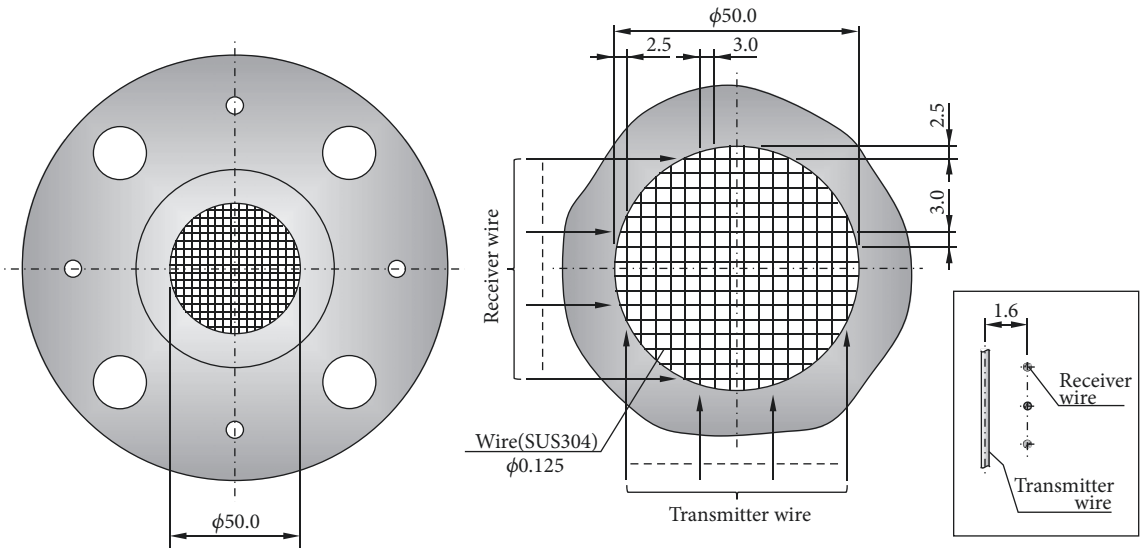

Figure 2: 16×16 grid sensor image to verify principle.

to increase the spatial resolution by decreasing the wire-to-wire distance, but since the influence of crosstalk increases, it is decided by balancing the influence of the wire-to-wire distance and crosstalk that can be practically realized from the dimensional point of view.

3.2. Experimental Apparatus. A schematic image of the 16×16 squared-grid sensor is illustrated in Figure 2. The transmitter and receiver wire electrodes are 125 μm in diameter and made of stainless (SUS304). The transmitter wire electrodes, a total of 16 of which are configured, are placed parallel to each other at 3 mm intervals. On another front, the receiver wire electrodes are placed parallel to each other and perpendicular to the transmitter wire electrodes at 1.6 mm intervals. The temperature profile of 256 spots (16×16) can be measured at a maximum of 5,000 Hz with the processing unit used in the apparatus. The grid sensor is employed for a mixing process test involving a hot-water jet directed into a cold pool.

Figure 3(a) expresses a schematic image of the 5×5 rod bundle geometry test loop. This apparatus comprises a circulation pump, flow meters, a preheater, the 5×5 bundle test section, a separation tank, and a condenser. The system pressure is atmospheric pressure and the test sample selected was ion-exchanged water. The electrical conductivity of the test sample should be steady and reproducible because this sensor measures electrical conductivity for temperature measurement. Details of the bundle section are explained in the following section, as well as Figure 3(b). The heated rod diameter is 10 mm and the rod pitch is 13 mm. The heated length is 2.0 m and its lower end is defined as a standard position (z = 0 mm). The rod bundle apparatus is installed in the polycarbonate container. Using this apparatus, experimental tests of calibration to confirm the principle and a three-dimensional temperature measurement in the bundle test section were demonstrated. The difficulty of the bundle testing device was to place a wire for the WMS in a 3 mm distance between the heated rods and installed with insulation resistance to the rod. In order to accurately measure the fluid temperature distribution in the bundle, it is essential to install the rod and the wire precisely at 1 mm intervals without touching each other.

4. Calibration Test

This chapter indicates verification of the relationship between electrical impedance with temperature and also compares measurement values with a conventional thermocouple in the bundle test loop. The bundle loop was adopted under non-heating conditions in the following experiments to regulate and maintain water temperature with the preheater and the cooler and to confirm the applicability of the temperature measurement in the bundle flow channel.

4.1. Detection of the Calibration Line. To confirm the relationship between water temperature and electrical impedance in the bundle test section, the signals were detected from the receiver wire electrode at a measurement spot. This chapter clarifies calibration trends regarding temperature versus electrical impedance, with electrical impedance signals of the measuring spot at 5 K intervals for 2 seconds indicated in Figure 4. The measuring height of the sensor and thermocouple is z = 598 mm. The calibration thermocouple was set flush on the right side of the center of the flow path. The point which is close to the thermocouple is adopted as the sensor measurement point for comparison in Figure 4. As previously noted, it can be confirmed that the water temperature is almost directly proportional to the electrical impedance of the receiver wire electrode in Figure 4 at atmospheric pressure region. The calibration line was defined from the time-averaged value under each condition. Subsequently, the absolute error at 90°C was 1.5 K against the averaged one, while that at 30°C was 3.7 K. The SN ratio of the detected signal provides measurement uncertainty. Although adding solute addition can improve

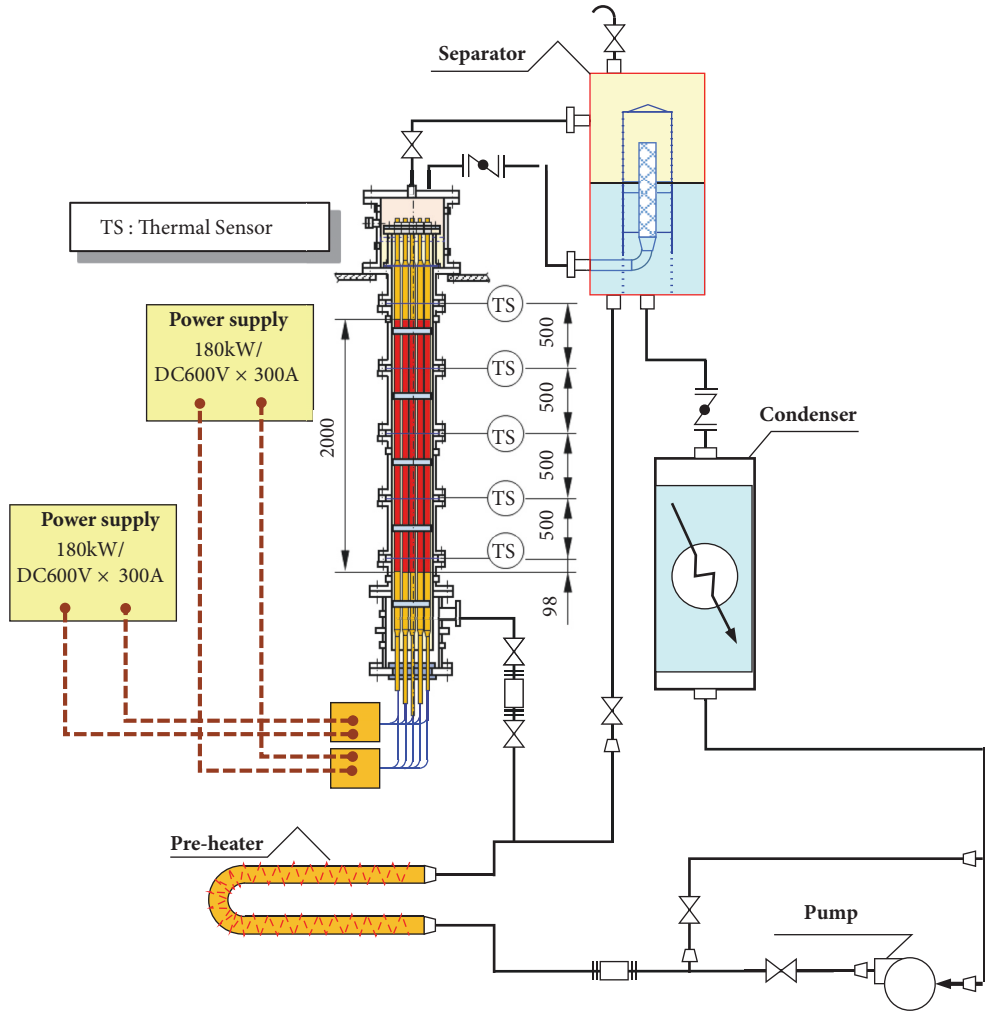

(a)

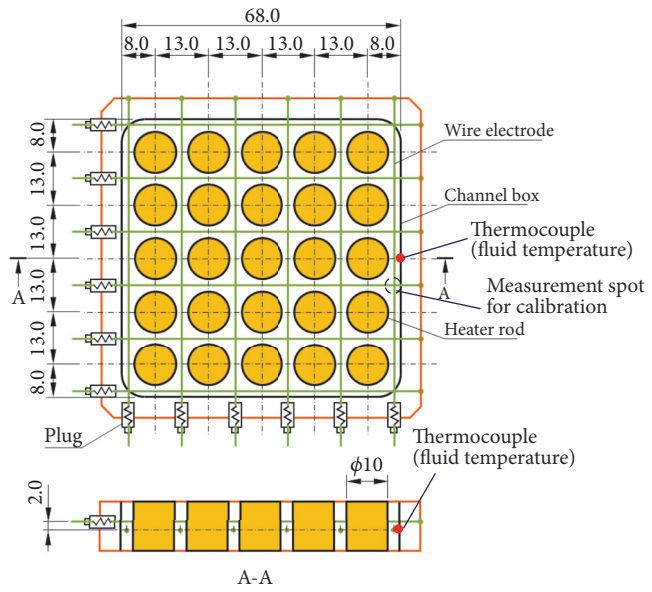

(b)

Figure 3: Experimental apparatus with 5×5 bundle geometry at z = 598 mm. (a) Main experimental contents, including the bundle test section. (b) Cross-sectional geometry of the temperature sensor.

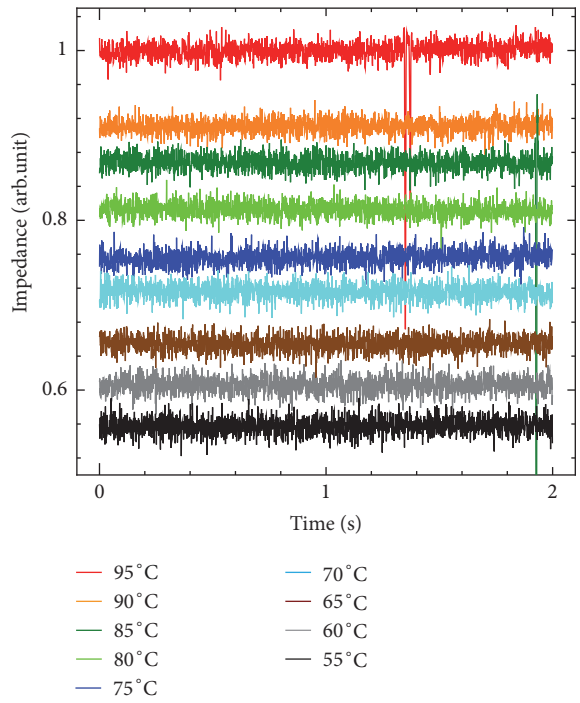

Figure 4: Temperature dependence trend on sensor signals.

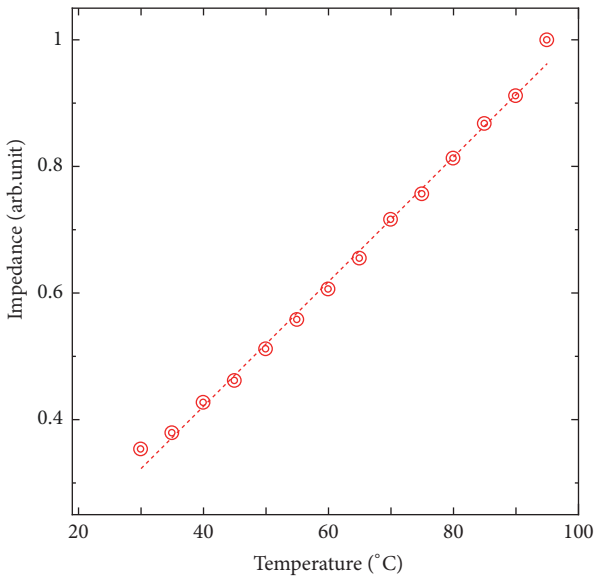

Figure 5: Linearization and calibration between the signals with temperature.

the SN ratio beyond that of pure water, given the inability to prevent variation in pH levels, this method is unsuitable for temperature measurement. Figure 5 illustrates the time-averaged electrical impedances under each temperature condition and their linearized calibration lines. If linearization can be assumed for the acquired temperature trend, which comprises the time-averaged spots, the gradient (dT/dV) and its intercept ($T_{int.}$) can be followed using the calibration line. With these parameters, the temporal temperature $T(t)$ of the water can be expressed through the following equation and,

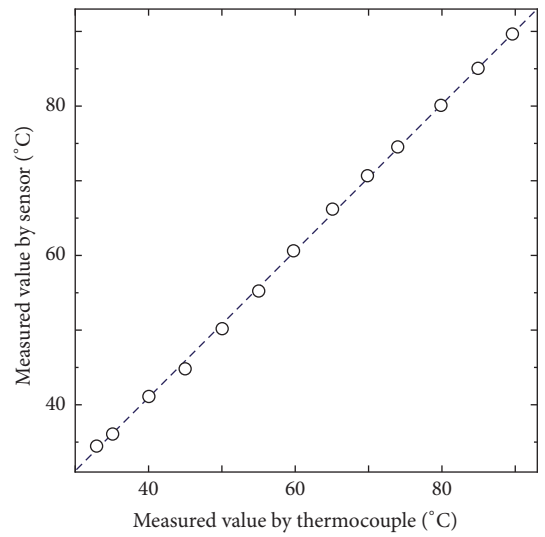

Figure 6: Comparison of a cooling flow process with a conventional thermocouple.

here, $V(t)$ is the temporal electrical impedance. With these two parameters, the temporal temperature $T(t)$ of the water can be expressed through the following equation, where $V(t)$ denotes temporal electrical impedance:

$$\mathrm{T}(t) = \left(\frac{dT}{dV}\right) \bullet V(t) + T_{int.} \quad (1)$$

In this experiment, these critical two parameters are detected from the time-averaged values which are measured at each of the detecting spots, respectively. The temperature of water, meanwhile, can be indirectly estimated from the wire electrode of each cross-measuring point.

4.2. Comparison with the Thermocouple in a Cooling Flow. This section compares the measurement temperatures between the sensors with a conventional thermocouple in a cooling flow to validate the temperature measurement technique. The difference from the previous section is that the temperature is continuously lowered and measured. It is a purpose to investigate whether temperature measurement is continuously possible from the preliminarily acquired calibration data in the previous section. The axial and cross-sectional geometries of the sensor section are shown schematically in Figures 3(a) and 3(b). The measuring height of the thermocouple is z = 598 mm as before, while that of the sensor is z =598 mm. The flow velocity was set at 0.2 m/s. This cooling test is prepared to increase the water temperature to 90°C near saturated temperature with the preheater. Subsequently, the coolant temperature was reduced using the condenser, whereupon the thermal behavior at a certain measuring point monitored both the grid sensor and the thermocouple.

Figure 6 illustrates comparative results recording the water temperature at the measuring point. Every time the thermometer reading at the inlet position of the test section declined by 5°C, the temperatures were measured with the sensor and thermocouple over 60 s. This figure expresses

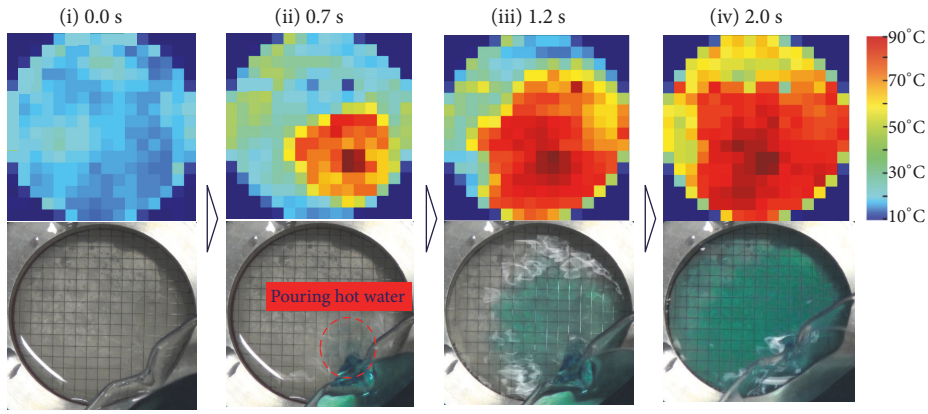

Figure 7: Mixing process of a hot-water jet into a cold-water pool.

the time-averaged values for 1 s, equating to a measuring frequency with both measurement techniques of 1000 Hz. It can be confirmed that the measuring values of the sensor correlated well to within ±15 % against that of the conventional technique in Figure 6. In this experiment, although the calibration expression adopted linear approximation, if curve approximation is selected, more precise measurement can be practiced. Here, we will describe the uncertainty factor in temperature measurement using the wire-mesh sensor. The measurement uncertainty of the thermocouple, the nonuniform conductivity within the inter-wire region (not considered uniform), the nonuniformity of the temperature field, and the stress applied to the wire by the flow are considered as factors behind the uncertainty. The measurement uncertainty of the thermocouple is ± 0.1°C as described in Section 3.1. In addition, a detailed discussion of other uncertainties will be omitted here because it differs from the application of WMSs targeting technical knowledge of cooling characteristics in nuclear reactors, which is the main point of this paper.

5. Results and Discussion

To confirm the measurement capabilities of time resolution performance and multidimensionality, two types of temperature measurement tests were demonstrated in this chapter with experimental apparatus of both nonflowing and flowing settings.

5.1. Mixing Process for Both Hot and Cold Water. The real-time measurement of the process of mixing a hot-water jet with a cold-water pool is demonstrated with a 16×16 grid sensor to confirm the speed performance of the sensor for core cooling in millisecond order. To enlarge the dynamic range of electrical impedance, the gain value of the detector is based on the signal value under the highest temperature condition in the experiment. To be precise, this criterion is set at 90 % of the saturation value for time-averaged electrical impedance. The sensor signal limit is 5 V and the signal at 90°C was set near 4.5 V. With a view to comparing the thermal behavior, visual observation was conducted using a video camera. A little methylene blue, in a negligible small region to avoid impacting on the physical properties, is added to the hot-water jet to visually clarify the hot-water jet and the cold-water pool.

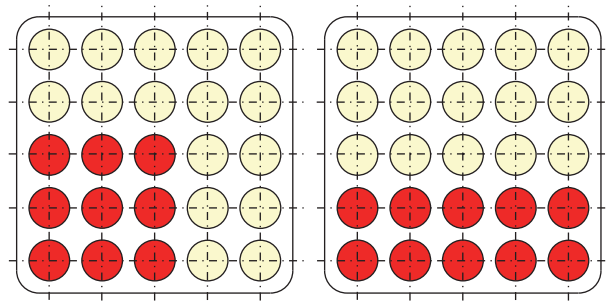

Figure 8: Heating pattern condition of the bundle geometry test.

The visualized images of the measured values with the 16×16 grid sensor and the photographs in the mixing process are illustrated over time in Figure 7, with the temperature values at each measuring point expressed via color contours from 10 to 90°C. Some chapter numbers indicated (i) before pouring, (ii) irrigation, (iii) after 0.5 seconds from irrigation, and (iv) finishing of irrigation, respectively. The pouring spot of the hot-water jet is conducted to the lower right of the photographs and the calculation process from electrical impedance to temperature was determined with a calibration line, itself predetermined from low (20°C) and high (95°C) conditions using a thermocouple. In Figure 7, it can be confirmed that the temperature variation was generated and spread from the lower right area in the two-dimensional profile. The wire-mesh temperature sensor can capture the temperature profile varied in the millisecond order to simulate core cooling in the reactor.

5.2. Three-Dimensional Gradient in Bundle Geometry. To measure the three-dimensional temperature profile in the bundle flow path for nuclear applications, a stationary heating test was conducted with the rod bundle loop apparatus and some heated rods were heated by applying a current. The radial and axial heat distributions of the rod bundle power are uniform. During the experiment, two heating patterns were demonstrated in Figure 8, each type of which is defined

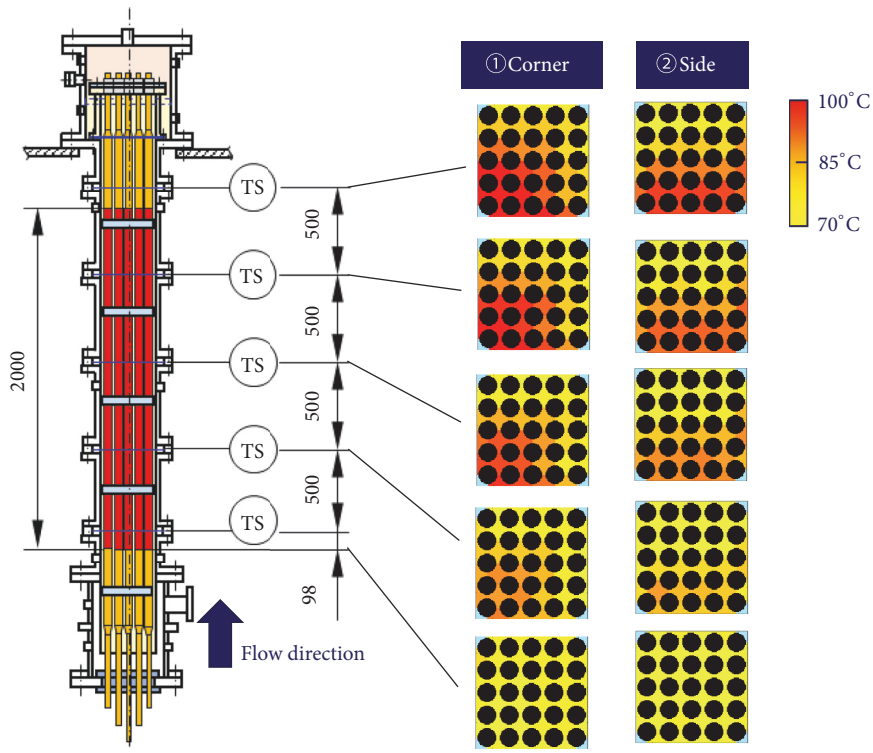

Figure 9: Visualized images of the sensor measurement signals.

in terms of corner and side types, respectively. The flow rate and inlet temperature were 70°C and 0.2 m/s and the bundle thermal power was decided at approximately 3 kW under a nonboiling condition to prevent boiling. Because the sensor method can detect only one-parameter in principle, bubbles tend to prevent temperature measurement. Visualization images of the measurement profiles are illustrated in Figure 9. Here the argyle region, which is framed by four-directional heated bundles, is known as the "sub-channel area" in the nuclear field. In the experiment, the measurement value at each crossed spot is defined as the representative subchannel area value and the temperature value at each measuring point has a color contour applied from 70 to 100°C. From the figure, it can be confirmed that the cross-sectional temperature distribution is the same as the heat generation distribution for each of the corner and side types and validity whereby the vertical temperature distribution increases toward the downstream side was shown. It was confirmed that three-dimensional temperature distribution measurement is possible in a bundle complex flow path and under a flow condition for nuclear reactor application. From the above, this sensor can also be applicable for measuring the temperature distribution of the core cooling process in a cold shutdown state in a nuclear reactor. Also, the use of stainless steel wires means it is also applicable to environments under high temperature and pressure.

6. Conclusions

Unsteady and multidimensional temperature distribution in nuclear reactor fuel assemblies is an important technical finding in nuclear reactor thermal hydraulics research. The purpose of this research was to expand knowledge of three-dimensional temperature distribution when injecting pure water during cold stoppage in LWR. To evaluate the cooling characteristics in the fuel assembly, a measurement method is required to capture the temperature distribution with high temporal and spatial resolution. Furthermore, if the pressure range can be applied up to the rated pressure 16 MPa of a pressurized water reactor (PWR), it is more practical. We applied the principle of the WMS technology to the temperature measurement and carried out a three-dimensional measurement of temperature distribution in the flow field, simulating the fuel assembly structure and the real-time measurement in the simulated transient thermal change process. The findings obtained below are shown:

(1) To confirm the measurement performance in bundle test section, an atmospheric pressure loop experimental apparatus with a 5 × 5 simulated fuel assembly as a test part was fabricated. It was shown that a predetermined temperature calibration line with respect to time-average impedance was calculated and became a function of temperature.

(2) To evaluate the followability of the temperature change in the transient process, we fabricated a 16 × 16 wire-mesh sensor device and measured the hot-water jet-mixing process into the cold-water pool in real time, whereupon the temperature profile was calculated from the temperature calibration line obtained in advance from each measurement point.

(3) To confirm the applicability to multidimensional temperature distribution measurement in a complicated flow field in the bundle, we demonstrated three-dimensional

temperature distribution measurement in the forced flow field with subcooling of 30°C when the 5×5 bundle was heated by energization.

Data Availability

The data used to support the findings of this study are available from the corresponding author upon request.

Conflicts of Interest

The authors declare that they have no conflicts of interest.

Acknowledgments

The authors would like to thank Messrs. Takeo Yoshioka and Tsugumasa Iiyama of Electric Power Engineering Systems Co. Ltd., for their help with these experiments.

References

[1] F. Wang, G.-W. Liang, and D.-L. Xie, "Research on the gas-holdup measurement of gas-liquid two-phase flow based on the dynamical differential pressure signals of multi-loop meter," *Chinese Journal of Sensors and Actuators*, vol. 20, no. 3, pp. 628–631, 2007.

[2] F. Chen and W. Liu, "Research on measurement of void fraction for vertically rising pipes by optical fiber probe," *Advanced Materials Research*, vol. 361-363, pp. 671–675, 2012.

[3] M. E. Shawkat, C. Y. Ching, and M. Shoukri, "On the liquid turbulence energy spectra in two-phase bubbly flow in a large diameter vertical pipe," *International Journal of Multiphase Flow*, vol. 33, no. 3, pp. 300–316, 2007.

[4] H.-M. Prasser, M. Misawa, and I. Tiseanu, "Comparison between wire-mesh sensor and ultra-fast X-ray tomograph for an air-water flow in a vertical pipe," *Flow Measurement and Instrumentation*, vol. 16, no. 2-3, pp. 73–83, 2005.

[5] S. Hosokawa and A. Tomiyama, "Bubble-induced pseudo turbulence in laminar pipe flows," *International Journal of Heat and Fluid Flow*, vol. 40, pp. 97–105, 2013.

[6] H.-M. Prasser, A. Böttger, and J. Zschau, "A new electrode-mesh tomograph for gas-liquid flows," *Flow Measurement and Instrumentation*, vol. 9, no. 2, pp. 111–119, 1998.

[7] T. Arai, M. Furuya, T. Kanai, and K. Shirakawa, "Development of a subchannel void sensor and two-phase flow measurement in 10×10 rod bundle," *International Journal of Multiphase Flow*, vol. 47, pp. 183–192, 2012.

[8] T. Arai, M. Furuya, T. Kanai, K. Shirakawa, and Y. Nishi, "Development of measurement method of void fraction distribution for boiling water flow in heated rod bundle," *Japanese Journal of Multiphase Flow*, vol. 27, no. 5, pp. 647–654, 2014.

[9] T. Kanai, M. Furuya, T. Arai, K. Shirakawa, and Y. Nishi, "Three-dimensional phasic velocity determination methods with wire-mesh sensor," *International Journal of Multiphase Flow*, vol. 46, pp. 75–86, 2012.

[10] J. Kickhofel, H.-M. Prasser, P. K. Selvam, E. Laurien, and R. Kulenovic, "T-junction cross-flow mixing with thermally driven density stratification," *Nuclear Engineering and Design*, vol. 309, pp. 23–39, 2016.

[11] R. M. Kowalik and C. H. Kruger, "Laser fluorescence temperature measurements," *Combustion and Flame*, vol. 34, no. C, pp. 135–140, 1979.